

---

# The $H_0$ tension in light of vacuum dynamics in the Universe

JOAN SOLÀ, ADRIÀ GÓMEZ-VALENT, JAVIER DE CRUZ PÉREZ

*Departament de Física Quàntica i Astrofísica, and Institute of Cosmos Sciences, Universitat de Barcelona, Av. Diagonal 647, E-08028 Barcelona, Catalonia, Spain*

PACS 98.80.-k – Cosmology  
PACS 95.36.+x – Dark Energy

**Abstract** – Despite the outstanding achievements of modern cosmology, the classical dispute on the precise value of  $H_0$ , which is the first ever parameter of modern cosmology and one of the prime parameters in the field, still goes on and on after over half a century of measurements. Recently the dispute came to the spotlight with renewed strength owing to the significant tension (at  $> 3\sigma$  c.l.) between the latest Planck determination obtained from the cosmic microwave background (CMB) anisotropies and the local measurement from the Hubble Space Telescope, based on Cepheid variables. In this Letter, we investigate the impact of the dynamical vacuum models (DVMs) on such a controversy. These models have been recently explored in great detail by us, see e.g. arXiv:1602.02103 and arXiv:1703.08218, where it is shown that by letting the vacuum energy to support a mild dynamical dependence on the cosmic expansion it is possible to strongly ameliorate the quality fit to the overall SNIa+BAO+ $H(z)$ +LSS+CMB cosmological observations, as compared to the concordance  $\Lambda$ CDM model. Here we show that the main DVMs can still surpass the  $\Lambda$ CDM fit even after including the local measurement of  $H_0$ , but our analysis definitely favors the CMB value. We find that even allowing a departure from the vacuum equation of state, the vacuum option  $w = -1$  continues to be preferred. The kind of cosmic vacuum that is favored, however, is *not* the traditional cosmological constant but a mildly evolving one,  $\rho_\Lambda(H(t))$ , as indicated above. The large scale structure (LSS) formation data play a momentous role in discriminating among the two options.

---

**Introduction.** – The most celebrated fact of modern observational cosmology is that the universe is in accelerated expansion [1, 2]. At the same time, the most paradoxical reality check is that we fully ignore the primary cause for such an acceleration. The simplest picture is to assume that it is caused by a strict cosmological term,  $\Lambda$ , in Einstein’s equations, but its fundamental origin is unknown [3]. Together with the assumption of the existence of dark matter (DM) and the spatial flatness of the Friedmann-Lemaître-Robertson-Walker (FLRW) metric (viz. the metric that expresses the homogeneity and isotropy inherent to the cosmological principle [4]), we are led to the “concordance”  $\Lambda$ CDM model, i.e. the standard model of cosmology. The model is consistent with a large body of observations, and in particular with the high precision data from the cosmic microwave background (CMB) anisotropies [5]. Many alternative explanations of the cosmic acceleration beyond a  $\Lambda$ -term are possible (including quintessence and the like, see e.g. the review [6]) and are called dark energy (DE) [7].

The current situation with cosmology is reminiscent of the prediction by the famous astronomer A. Sandage in the sixties, who asserted that the main task of future observational cosmology would be the search for two parameters: the Hubble constant  $H_0$  and the deceleration parameter  $q_0$  [8]. The first of them is the most important distance (and time) scale in cosmology prior to any other cosmological quantity. Sandage’s last published value with Tammann (in 2010) is 62.3 km/s/Mpc [9] – slightly revised in Ref. [10] as  $H_0 = 64.1 \pm 2.4$  km/s/Mpc. There is currently a significant tension between CMB measurements of  $H_0$  [5, 11] – not far away from this value – and local determinations emphasizing a higher range above 70 km/s/Mpc [12, 13]. As for  $q_0$ , its measurement is tantamount to determining  $\Lambda$  in the context of the concordance model. On fundamental grounds, however, understanding the value of  $\Lambda$  is not just a matter of observation; in truth and in fact, it embodies one of the most important and unsolved conundrums of theoretical physics and cosmology: the cosmological constant problem, see e.g. [3, 6, 14, 15]. The problem is con-

nected to the fact that the  $\Lambda$ -term is usually associated with the vacuum energy density,  $\rho_\Lambda = \Lambda/(8\pi G)$ , with  $G$  Newton's coupling. The prediction for  $\rho_\Lambda$  in quantum field theory (QFT) exceeds the measured value  $\rho_\Lambda \sim 10^{-47}$  GeV<sup>4</sup> (in natural units  $c = \hbar = 1$ ) by many orders of magnitude [15].

Concerning the prime parameter  $H_0$ , the tension among the different measurements is inherent to its long and tortuous history. Let us only recall that after Baade's revision (by a factor of one half [16]) of the exceedingly large value  $\sim 500$  km/s/Mpc originally estimated by Hubble (which implied a universe of barely two billion years old only), the Hubble parameter was subsequently lowered to 75 km/s/Mpc and finally to  $H_0 = 55 \pm 5$  km/s/Mpc, where it remained for 20 years (until 1995), mainly under the influence of Sandage's devoted observations [17]. Shortly after that period the first measurements of the nonvanishing, positive, value of  $\Lambda$  appeared [1, 2] and the typical range for  $H_0$  moved upwards to  $\sim 65$  km/s/Mpc. In the meantime, many different observational values of  $H_0$  have piled up in the literature using different methods (see e.g. the median statistical analysis of  $> 550$  values considered in [18, 19]). As mentioned above, two kinds of *precision* (few percent level) measurements of  $H_0$  have generated considerable perplexity in the recent literature, specifically between the latest Planck values obtained from the CMB anisotropies, and the local measurement from the Hubble Space Telescope (HST), based on distance estimates from Cepheids. The latter reads  $H_0 = 73.24 \pm 1.74$  km/s/Mpc [12], which can be compared with the CMB value  $H_0 = 67.51 \pm 0.64$  km/s/Mpc, as extracted from Planck 2015 TT,TE,EE+lowP+lensing data [5], or with  $H_0 = 66.93 \pm 0.62$  km/s/Mpc, based on Planck 2015 TT,TE,EE+SIMlow data [11]. In both cases there is a tension above  $3\sigma$  c.l. (viz.  $3.1\sigma$  and  $3.4\sigma$ , respectively) with respect to the local measurement. This situation, and in general a certain level of tension with some independent observations in intermediate cosmological scales, has stimulated a number of discussions and possible solutions in the literature, see e.g. [20–25].

We wish to examine here the problem of the  $H_0$  tension, but not as an isolated strain between two particular sources of observations, but rather in light of the overall fit to the cosmological data SNIa+BAO+ $H(z)$ +LSS+CMB. Recently, it has been demonstrated that by letting the cosmological vacuum energy density to slowly evolve with the expansion rate,  $\rho_\Lambda = \rho_\Lambda(H)$ , the global fit can be improved with respect to the  $\Lambda$ CDM at a confidence level of  $3-4\sigma$  [26–30]. We devote this Letter to show that the dynamical vacuum models (DVMS) can still give a better fit to the overall data, even if the recent local measurement of the Hubble parameter is taken into account. However we find that our best-fit values of  $H_0$  are much closer to the value extracted from CMB measurements [5, 11]. Our analysis corroborates that the large scale structure formation data (LSS) are crucial in distinguishing the rigid vacuum option from the dynamical one.

**Dynamical vacuum models and beyond.** – Let us consider a generic cosmological framework described by the spatially flat FLRW metric, in which matter is exchanging energy with a dynamical DE medium with a phenomenological equation of state (EoS)  $p_\Lambda = w\rho_\Lambda$ , where  $w = -1 + \epsilon$  (with  $|\epsilon| \ll 1$ ). Such medium is therefore of quasi-vacuum type, and for  $w = -1$  (i.e.  $\epsilon = 0$ ) we precisely recover the genuine vacuum case. Owing, however, to the exchange of energy with matter,  $\rho_\Lambda = \rho_\Lambda(\zeta)$  is in all cases a *dynamical* function that depends on a cosmic variable  $\zeta = \zeta(t)$ . We will identify the nature of  $\zeta(t)$  later on, but its presence clearly indicates that  $\rho_\Lambda$  is no longer associated to a strictly rigid cosmological constant as in the  $\Lambda$ CDM. The Friedmann and acceleration equations read, however, formally identical to the standard case:

$$3H^2 = 8\pi G (\rho_m + \rho_r + \rho_\Lambda(\zeta)) \quad (1)$$

$$3H^2 + 2\dot{H} = -8\pi G (p_r + p_\Lambda(\zeta)). \quad (2)$$

Here  $H = \dot{a}/a$  is the Hubble function,  $a(t)$  the scale factor as a function of the cosmic time,  $\rho_r$  is the energy density of the radiation component (with pressure  $p_r = \rho_r/3$ ), and  $\rho_m = \rho_b + \rho_{dm}$  involves the contributions from baryons and cold DM. The local conservation law associated to the above equations reads:

$$\dot{\rho}_r + 4H\rho_r + \dot{\rho}_m + 3H\rho_m = Q, \quad (3)$$

where

$$Q = -\dot{\rho}_\Lambda - 3H(1+w)\rho_\Lambda. \quad (4)$$

For  $w = -1$  the latter boils down to  $Q = -\dot{\rho}_\Lambda$ , which is nonvanishing since  $\dot{\rho}_\Lambda \neq 0$  on account of  $\rho_\Lambda(t) = \rho_\Lambda(\zeta(t))$ .

The simplest case is, of course, that of the concordance model, in which  $\rho_\Lambda = \rho_{\Lambda 0} = \text{const}$  and  $w = -1$ , so that  $Q = 0$  trivially. However, for  $w \neq -1$  we can also have  $Q = 0$  in a nontrivial situation, which follows from solving Eq. (4). It corresponds to the XCDM parametrization [32], in which the DE density is dynamical and self-conserved. It is easily found in terms of the scale factor:

$$\rho_\Lambda^{XCDM}(a) = \rho_{\Lambda 0} a^{-3(1+w)} = \rho_{\Lambda 0} a^{-3\epsilon}, \quad (5)$$

where  $\rho_{\Lambda 0}$  is the current value. From (3) it then follows that the matter component is also conserved, meaning that after equality it leads to separate conservation of cold matter and radiation. In general,  $Q$  can be a nonvanishing interaction source allowing energy exchange between matter and the quasi-vacuum medium under consideration;  $Q$  can either be given by hand (i.e. it can be an *ad hoc* ansatz), or can be suggested by a particular theoretical framework. In any case the interaction source must satisfy  $0 < |Q| \ll \dot{\rho}_m$  since we do not wish to depart too much from the concordance model. Despite matter is exchanging energy with the quasi-vacuum medium, we shall assume that radiation and baryons are separately self-conserved, i.e.  $\dot{\rho}_r + 4H\rho_r = 0$  and  $\dot{\rho}_b + 3H\rho_b = 0$ , so that their energy densities evolve in the standard way:

Model	$h$	$\omega_b$	$n_s$	$\Omega_m^0$	$\nu_i$	$w$	$\chi_{\min}^2/dof$	$\Delta AIC$	$\Delta BIC$
$\Lambda$ CDM	$0.688 \pm 0.004$	$0.02243 \pm 0.00013$	$0.973 \pm 0.004$	$0.298 \pm 0.004$	-	-	84.40/85	-	-
XCDM	$0.672 \pm 0.006$	$0.02251 \pm 0.00013$	$0.975 \pm 0.004$	$0.311 \pm 0.006$	-	$-0.936 \pm 0.023$	76.80/84	5.35	3.11
RVM	$0.674 \pm 0.005$	$0.02224 \pm 0.00014$	$0.964 \pm 0.004$	$0.304 \pm 0.005$	$0.00158 \pm 0.00042$	-	68.67/84	13.48	11.24
$Q_{dm}$	$0.675 \pm 0.005$	$0.02222 \pm 0.00014$	$0.964 \pm 0.004$	$0.304 \pm 0.005$	$0.00218 \pm 0.00057$	-	69.13/84	13.02	10.78
$Q_\Lambda$	$0.688 \pm 0.003$	$0.02220 \pm 0.00015$	$0.964 \pm 0.005$	$0.299 \pm 0.004$	$0.00673 \pm 0.00236$	-	76.30/84	5.85	3.61
$w$ RVM	$0.671 \pm 0.007$	$0.02228 \pm 0.00016$	$0.966 \pm 0.005$	$0.307 \pm 0.007$	$0.00140 \pm 0.00048$	$-0.979 \pm 0.028$	68.15/83	11.70	7.27
$wQ_{dm}$	$0.670 \pm 0.007$	$0.02228 \pm 0.00016$	$0.966 \pm 0.005$	$0.308 \pm 0.007$	$0.00189 \pm 0.00066$	$-0.973 \pm 0.027$	68.22/83	11.63	7.20
$wQ_\Lambda$	$0.671 \pm 0.007$	$0.02227 \pm 0.00016$	$0.965 \pm 0.005$	$0.313 \pm 0.006$	$0.00708 \pm 0.00241$	$-0.933 \pm 0.022$	68.24/83	11.61	7.18

Table 1: Best-fit values for  $\Lambda$ CDM, XCDM the three dynamical vacuum models (DVMS) and the three dynamical dark energy models ( $w$ DVMS), including their statistical significance ( $\chi^2$ -test and Akaike and Bayesian information criteria AIC and BIC). For detailed description of the data and a full list of references, see [27] and [30]. The quoted number of degrees of freedom ( $dof$ ) is equal to the number of data points minus the number of independent fitting parameters (4 for the  $\Lambda$ CDM, 5 for the XCDM and the DVMS, and 6 for the  $w$ DVMS). For the CMB data we have used the marginalized mean values and covariance matrix for the parameters of the compressed likelihood for Planck 2015 TT,TE,EE + lowP+ lensing data from [31]. Each best-fit value and the associated uncertainties have been obtained by marginalizing over the remaining parameters.

Model	$h$	$\omega_b$	$n_s$	$\Omega_m^0$	$\nu_i$	$w$	$\chi_{\min}^2/dof$	$\Delta AIC$	$\Delta BIC$
$\Lambda$ CDM	$0.690 \pm 0.003$	$0.02247 \pm 0.00013$	$0.974 \pm 0.003$	$0.296 \pm 0.004$	-	-	90.59/86	-	-
XCDM	$0.680 \pm 0.006$	$0.02252 \pm 0.00013$	$0.975 \pm 0.004$	$0.304 \pm 0.006$	-	$-0.960 \pm 0.023$	87.38/85	0.97	-1.29
RVM	$0.679 \pm 0.005$	$0.02232 \pm 0.00014$	$0.967 \pm 0.004$	$0.300 \pm 0.004$	$0.00133 \pm 0.00040$	-	78.96/85	9.39	7.13
$Q_{dm}$	$0.679 \pm 0.005$	$0.02230 \pm 0.00014$	$0.966 \pm 0.004$	$0.300 \pm 0.004$	$0.00185 \pm 0.00057$	-	79.17/85	9.18	6.92
$Q_\Lambda$	$0.690 \pm 0.003$	$0.02224 \pm 0.00016$	$0.965 \pm 0.005$	$0.297 \pm 0.004$	$0.00669 \pm 0.00234$	-	82.48/85	5.87	3.61
$w$ RVM	$0.680 \pm 0.007$	$0.02230 \pm 0.00015$	$0.966 \pm 0.005$	$0.300 \pm 0.006$	$0.00138 \pm 0.00048$	$-1.005 \pm 0.028$	78.93/84	7.11	2.66
$wQ_{dm}$	$0.679 \pm 0.007$	$0.02230 \pm 0.00016$	$0.966 \pm 0.005$	$0.300 \pm 0.006$	$0.00184 \pm 0.00066$	$-0.999 \pm 0.028$	79.17/84	6.88	2.42
$wQ_\Lambda$	$0.679 \pm 0.006$	$0.02227 \pm 0.00016$	$0.966 \pm 0.005$	$0.306 \pm 0.006$	$0.00689 \pm 0.00237$	$-0.958 \pm 0.022$	78.98/84	7.07	2.61

Table 2: The same as Table 1 but adding the  $H_0$  local measurement from [12].

$\rho_r(a) = \rho_{r0} a^{-4}$  and  $\rho_b(a) = \rho_{b0} a^{-3}$ . The dynamics of  $\rho_\Lambda$  can therefore be associated to the exchange of energy exclusively with the DM (through the nonvanishing source  $Q$ ) and/or with the possibility that the DE medium is not exactly the vacuum,  $w \neq -1$ , but close to it  $|\epsilon| \ll 1$ . Under these conditions, the coupled system of conservation equations (3)-(4) reduces to

$$\dot{\rho}_{dm} + 3H\rho_{dm} = Q \quad (6)$$

$$\dot{\rho}_\Lambda + 3H\epsilon\rho_\Lambda = -Q. \quad (7)$$

In the following we shall for definiteness focus our study of the dynamical vacuum and quasi-vacuum models to the three interactive sources:

$$\text{Model I (}w\text{RVM)} : Q = \nu H(3\rho_m + 4\rho_r) \quad (8)$$

$$\text{Model II (}wQ_{dm}) : Q_{dm} = 3\nu_{dm}H\rho_{dm} \quad (9)$$

$$\text{Model III (}wQ_\Lambda) : Q_\Lambda = 3\nu_\Lambda H\rho_\Lambda. \quad (10)$$

Here  $\nu_i = \nu, \nu_{dm}, \nu_\Lambda$  are small dimensionless constants,  $|\nu_i| \ll 1$ , which are determined from the overall fit to the data, see e.g. Tables 1 and 2. The ordinal number names I,II and III will be used for short, but the three model names are preceded by  $w$  to recall that, in the general case, the equation of state (EoS) is near the vacuum one (that is,  $w = -1 + \epsilon$ ). These dynamical DE models are also denoted as  $w$ DVMS. In the special case  $w = -1$  (i.e.  $\epsilon = 0$ ) we recover the dynamical vacuum models (DVMS), which were previously studied in detail in [30], and in this case the names of the models will not be preceded by  $w$ .

For all the above DVMS the cosmic variable  $\zeta$  can be taken to be the scale factor,  $\zeta = a(t)$ , since they are all analytically solvable in terms of it, as we shall see in a

moment. However, Model I is the running vacuum model (RVM), see [15, 29, 30, 33]. It is special in that the interaction source indicated in (8) is not *ad hoc* but follows from a dynamical vacuum energy expression  $\rho_\Lambda(\zeta)$  in which  $\zeta$  is not just the scale factor but the full Hubble rate:  $\zeta = H(a)$ . The explicit RVM form reads

$$\rho_\Lambda(H) = \frac{3}{8\pi G} (c_0 + \nu H^2). \quad (11)$$

The additive constant  $c_0 = H_0^2 (\Omega_\Lambda^0 - \nu)$  is fixed by the boundary condition  $\rho_\Lambda(H_0) = \rho_{\Lambda 0}$ , being  $\rho_{\Lambda 0}$  and  $\Omega_\Lambda^0$  the current values. Combining the field equations (1)-(2), we find  $\dot{H} = -(4\pi G/3)(3\rho_m + 4\rho_r + 3\epsilon\rho_\Lambda)$ , and upon differentiating (11) with respect to the cosmic time we are led to  $\dot{\rho}_\Lambda = -\nu H(3\rho_m + 4\rho_r + 3\epsilon\rho_\Lambda)$ . Thus, for  $\epsilon = 0$  (vacuum case)  $\dot{\rho}_\Lambda = -Q$  for  $Q$  of the form (8). However, for the quasi-vacuum case ( $0 < |\epsilon| \ll 1$ ) Eq. (7) does not strictly hold if  $\rho_\Lambda(H)$  adopts the RVM form (11). This form is thus specific to the pure vacuum EoS, and it can be related to a renormalization group equation for  $\rho_\Lambda(H)$ , which explains the RVM name. In it  $\nu$  plays the role of  $\beta$ -function coefficient for the running of  $\rho_\Lambda$  with the Hubble rate. Thus, we naturally expect  $|\nu| \ll 1$  in QFT, see [15, 34]. Models II and III are phenomenological models in which the interaction source  $Q$  is introduced by hand, see also the studies [25, 35-37] and references therein. The RVM vacuum form (11) has a QFT motivation and can actually be extended with higher powers of  $H^n$  (typically  $n = 4$ ) to provide an effective description of the cosmic evolution starting from the inflationary universe up to our days [33, 38].

The energy densities for the  $w$ DVMS can be computed

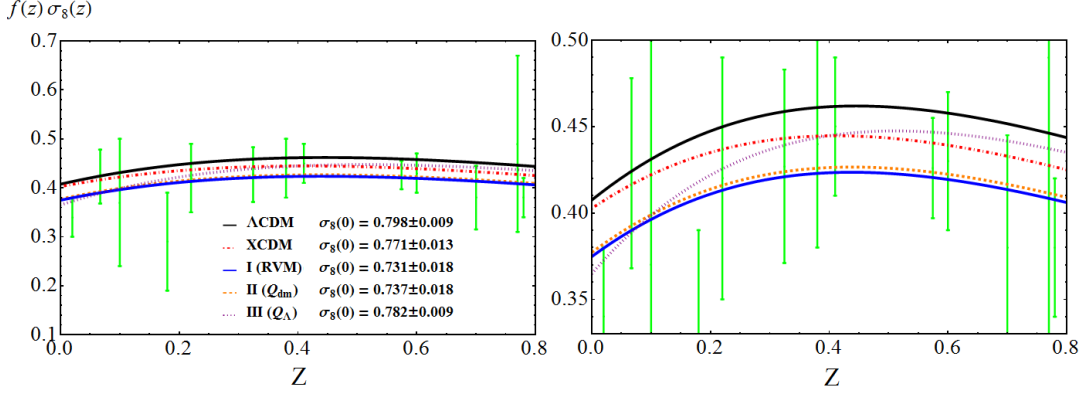


Fig. 1: **Left:** The LSS structure formation data ( $f(z)\sigma_8(z)$ ) versus the predicted curves by Models I, II and III, see equations (8)-(10) for the case  $w = -1$ , i.e. the dynamical vacuum models (DVMs), using the best-fit values in Table 1. The XCDM curve is also shown. The values of  $\sigma_8(0)$  that we obtain for the models are also indicated. **Right:** Zoomed window of the plot on the left, which allows to better distinguish the various models.

straightforwardly. For simplicity, we shall quote the leading parts only. The exact formulas containing the radiation terms are more cumbersome. In the numerical analysis we have included the full expressions. Details will be shown elsewhere. For the matter densities, we find

$$\begin{aligned}\rho_{dm}^I(a) &= \rho_{dm0} a^{-3(1-\nu)} + \rho_{b0} \left( a^{-3(1-\nu)} - a^{-3} \right) \\ \rho_{dm}^{II}(a) &= \rho_{dm0} a^{-3(1-\nu_{dm})} \\ \rho_{dm}^{III}(a) &= \rho_{dm0} a^{-3} + \frac{\nu_\Lambda}{\nu_\Lambda + w} \rho_{\Lambda0} \left( a^{-3} - a^{-3(\epsilon+\nu_\Lambda)} \right),\end{aligned}\quad (12)$$

and for the quasi-vacuum DE densities:

$$\begin{aligned}\rho_\Lambda^I(a) &= \rho_{\Lambda0} a^{-3\epsilon} - \frac{\nu \rho_{m0}}{\nu + w} \left( a^{-3(1-\nu)} - a^{-3\epsilon} \right) \\ \rho_\Lambda^{II}(a) &= \rho_{\Lambda0} a^{-3\epsilon} - \frac{\nu_{dm} \rho_{dm0}}{\nu_{dm} + w} \left( a^{-3(1-\nu_{dm})} - a^{-3\epsilon} \right) \\ \rho_\Lambda^{III}(a) &= \rho_{\Lambda0} a^{-3(\epsilon+\nu_\Lambda)}.\end{aligned}\quad (13)$$

Two specific dimensionless parameters enter each formula,  $\nu_i = (\nu, \nu_{dm}, \nu_\Lambda)$  and  $w = -1 + \epsilon$ . They are part of the fitting vector of free parameters for each model, as explained in detail in the caption of Table 1. For  $\nu_i \rightarrow 0$  the models become non interactive and they all reduce to the XCDM model case (5). For  $w = -1$  we recover the DVMs results previously studied in [30]. Let us also note that for  $\nu_i > 0$  the vacuum decays into DM (which is thermodynamically favorable) whereas for  $\nu_i < 0$  is the other way around. When  $w$  enters the fit,  $\epsilon$  tends to be larger than  $\nu_i$ , e.g. we have  $\epsilon = \mathcal{O}(10^{-2})$  and  $\nu_i = \mathcal{O}(10^{-3})$  in Table 1. For Models I and II the fit quality does not improve as compared to the  $\epsilon = 0$  case. It only improves for Model III. The three  $w$ DVMs actually become leveled. For  $\epsilon > 0$  the behavior is quintessence-like and for  $\epsilon < 0$  is phantom-like. The last case occurs in Table 2 and specially in Table 3.

Given the energy densities (12) and (13), the Hubble function immediately follows. For example, for Model I:

$$H^2(a) = H_0^2 \left[ a^{-3\epsilon} + \frac{w}{w + \nu} \Omega_m^0 \left( a^{-3(1-\nu)} - a^{-3\epsilon} \right) \right]. \quad (14)$$

Similar formulas can be obtained for Models II and III. For  $w = -1$  they all reduce to the DVM forms previously found in [30]. And of course they all finally boil down to the  $\Lambda$ CDM form in the limit  $w \rightarrow -1$  and  $\nu_i \rightarrow 0$ .

#### Structure formation: the role of the LSS data. –

The analysis of structure formation plays a crucial role in the fitting results. For the  $\Lambda$ CDM and XCDM we use the standard perturbations equation [4]

$$\ddot{\delta}_m + 2H \dot{\delta}_m - 4\pi G \rho_m \delta_m = 0, \quad (15)$$

with, however, the Hubble function corresponding to each one of these models. For the  $w$ DVMs, a step further is needed: the perturbation equation not only involves the modified Hubble function but the equation itself becomes modified. Trading the cosmic time for the scale factor and extending the analysis of [30, 39, 40] for  $w \neq -1$  ( $\epsilon \neq 0$ ), we find

$$\delta_m'' + \frac{A(a)}{a} \delta_m' + \frac{B(a)}{a^2} \delta_m = 0, \quad (16)$$

where the prime denotes differentiation with respect to the scale factor, and the functions  $A(a)$  and  $B(a)$  read

$$A(a) = 3 + \frac{aH'}{H} + \frac{\Psi}{H} - 3r\epsilon \quad (17)$$

$$\begin{aligned}B(a) &= -\frac{4\pi G \rho_m}{H^2} + 2\frac{\Psi}{H} + \frac{a\Psi'}{H} - 15r\epsilon \\ &\quad - 9\epsilon^2 r^2 + 3\epsilon(1+r)\frac{\Psi}{H} - 3r\epsilon\frac{aH'}{H}.\end{aligned}\quad (18)$$

Here  $r \equiv \rho_\Lambda/\rho_m$  and  $\Psi \equiv -\dot{\rho}_\Lambda/\rho_m$ . For  $\nu_i = 0$  we have  $\Psi = 3Hr\epsilon$ , and Eq. (16) can be brought back to the common one for the XCDM and  $\Lambda$ CDM, Eq. (15).

To solve the above perturbation equations we have to fix the initial conditions on  $\delta_m$  and  $\delta_m'$  for each model at high redshift, namely when non-relativistic matter dominates over radiation and DE, see [30]. In this regime, functions (17) and (18) behave approximately constant and Eq. (16)

Model	$h$	$\omega_b$	$n_s$	$\Omega_m^0$	$\nu_i$	$w$	$\chi_{\min}^2/dof$	$\Delta AIC$	$\Delta BIC$
$\Lambda$ CDM	$0.682 \pm 0.004$	$0.02234 \pm 0.00013$	$0.968 \pm 0.004$	$0.306 \pm 0.005$	-	-	13.85/11	-	-
RVM	$0.677 \pm 0.007$	$0.02227 \pm 0.00016$	$0.965 \pm 0.005$	$0.306 \pm 0.005$	$0.0010 \pm 0.0010$	-	13.02/10	-3.84	-1.88
$Q_\Lambda$	$0.683 \pm 0.004$	$0.02226 \pm 0.00016$	$0.965 \pm 0.005$	$0.305 \pm 0.005$	$0.0030 \pm 0.0030$	-	12.91/10	-3.73	-1.77
$w$ RVM	$0.663 \pm 0.023$	$0.02228 \pm 0.00016$	$0.966 \pm 0.005$	$0.313 \pm 0.012$	$0.0017 \pm 0.0016$	$-0.956 \pm 0.071$	12.65/9	-9.30	-4.22
$wQ_\Lambda$	$0.667 \pm 0.018$	$0.02226 \pm 0.00016$	$0.965 \pm 0.005$	$0.317 \pm 0.014$	$0.0070 \pm 0.0054$	$-0.921 \pm 0.082$	12.06/9	-8.71	-3.63
$\Lambda$ CDM*	$0.685 \pm 0.004$	$0.02239 \pm 0.00013$	$0.969 \pm 0.004$	$0.303 \pm 0.005$	-	-	21.76/12	-	-
RVM*	$0.685 \pm 0.007$	$0.02240 \pm 0.00015$	$0.969 \pm 0.005$	$0.303 \pm 0.005$	$0.0000 \pm 0.0010$	-	21.76/11	-4.36	-2.77
$Q_\Lambda^*$	$0.686 \pm 0.004$	$0.02224 \pm 0.00016$	$0.966 \pm 0.005$	$0.302 \pm 0.005$	$0.0034 \pm 0.0030$	-	20.45/11	-3.05	-1.46
Ia ( $w$ RVM*)	$0.709 \pm 0.015$	$0.02231 \pm 0.00016$	$0.967 \pm 0.005$	$0.290 \pm 0.008$	$-0.0008 \pm 0.0010$	$-1.094 \pm 0.050$	18.03/10	-5.97	-1.82
IIIa ( $wQ_\Lambda^*$ )	$0.703 \pm 0.013$	$0.02228 \pm 0.00016$	$0.966 \pm 0.005$	$0.291 \pm 0.010$	$-0.0006 \pm 0.0042$	$-1.086 \pm 0.065$	18.64/10	-6.58	-2.43

Table 3: Best-fit values for the  $\Lambda$ CDM and models RVM,  $Q_\Lambda$ ,  $w$ RVM and  $wQ_\Lambda$  by making use of the CMB+BAO data only. In contrast to Tables 1-2, we fully exclude now the LSS data (see [27, 30] for the complete reference list) to test its effect. The starred/non-starred cases correspond respectively to adding or not the local value for  $H_0$  from [12] as data point in the fit. The AIC and BIC differences of the starred models are computed with respect to the  $\Lambda$ CDM\*. We can see that all scenarios in this table are unfavored:  $\Delta AIC, \Delta BIC < 0$ . See the text for further details.

admits power-law solutions  $\delta_m(a) = a^s$ . The values of  $s$  for each model are computed to be

$$\begin{aligned}
 s^I &= 1 + \frac{3}{5}\nu \left( \frac{1}{w} - 4 \right) + \mathcal{O}(\nu^2) \\
 s^{II} &= 1 - \frac{3}{5}\nu_{dm} \left( 1 + 3 \frac{\Omega_{dm}^0}{\Omega_m^0} - \frac{1}{w} \right) + \mathcal{O}(\nu_{dm}^2) \\
 s^{III} &= 1.
 \end{aligned} \tag{19}$$

Once more we can check that for  $w = -1$  all of the above equations furnish the results of [30].

The analysis of the linear LSS regime is usually implemented with the help of the weighted linear growth  $f(z)\sigma_8(z)$ , where  $f(z) = d \ln \delta_m / d \ln a$  is the growth factor and  $\sigma_8(z)$  is the rms mass fluctuation on  $R_8 = 8 h^{-1}$  Mpc scales. It is computed as follows:

$$\sigma_8(z) = \sigma_{8,\Lambda} \frac{\delta_m(z)}{\delta_m^\Lambda(0)} \sqrt{\frac{\int_0^\infty k^{n_s+2} T^2(\vec{p}, k) W^2(kR_8) dk}{\int_0^\infty k^{n_{s,\Lambda}+2} T^2(\vec{p}_\Lambda, k) W^2(kR_{8,\Lambda}) dk}}, \tag{20}$$

where  $W$  is a top-hat smoothing function and  $T(\vec{p}, k)$  the transfer function (see e.g. [27, 30] for details). The fitting parameters for each model are contained in  $\vec{p}$ . Following these references, we have defined as fiducial model the  $\Lambda$ CDM at fixed parameter values from the Planck 2015 TT,TE,EE+lowP+lensing data [5]. These fiducial values are collected in  $\vec{p}_\Lambda$ . In Fig. 1-2 we display  $f(z)\sigma_8(z)$  for the various models using the fitted values of Tables 1-3. We note that our BAO and LSS data include the bispectrum data points from [41], see [30] for a detailed explanation of our data sets. In the next section we discuss the obtained results for the various models and assess their ability to improve the  $\Lambda$ CDM fit.

**Discussion.** – Following [30] (see Appendix B in it) the statistical analysis of the various models is performed in terms of a joint likelihood function, which is the product of the likelihoods for each data source and including the corresponding covariance matrices. As indicated in the caption of Table 1, the  $\Lambda$ CDM has 4 parameters, whereas XCDM and the DVMS have 5, and finally any  $w$ DVM has 6. Thus, for a fairer comparison of the various non-standard models with the concordance  $\Lambda$ CDM we have to

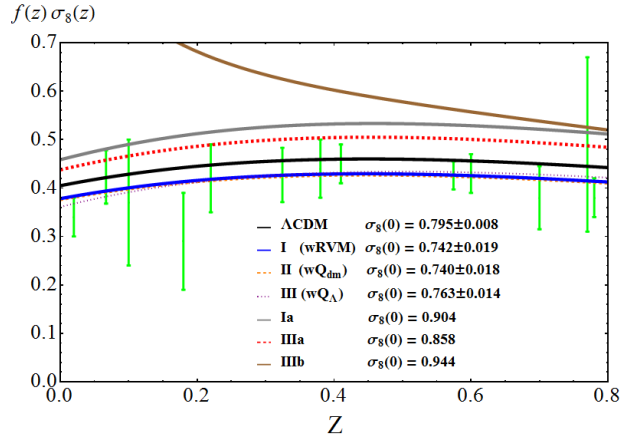


Fig. 2: The LSS structure formation data ( $f(z)\sigma_8(z)$ ) and the theoretical predictions for models (8)-(10), using the best-fit values in Tables 2 and 3. The curves for the cases Ia, IIIa correspond to special scenarios for Models I and III where the agreement with the Riess et al. local value of  $H_0$  is better (cf. Table 3). The price, however, is that the concordance with the LSS data is now spoiled. Case IIIb is our theoretical prediction for the scenario proposed in [25], aimed at optimally relaxing the  $H_0$  tension with Riess et al. [12]. The last three scenarios lead to phantom-like DE and are in serious disagreement with the LSS data.

invoke efficient criteria in which the presence of extra parameters in a given model is conveniently penalized so as to achieve a balanced comparison with the model having less parameters. The Akaike information criterion (AIC) and the Bayesian information criterion (BIC) are known to be extremely valuable tools for a fair statistical analysis of this kind. They can be thought of as a modern quantitative formulation of Occam’s razor. They read [42–45]:

$$AIC = \chi_{\min}^2 + \frac{2nN}{N - n - 1}, \quad BIC = \chi_{\min}^2 + n \ln N, \tag{21}$$

where  $n$  is the number of independent fitting parameters and  $N$  the number of data points. The bigger are the differences  $\Delta AIC$  and  $\Delta BIC$  with respect to the model having smaller values of AIC and BIC the higher is the evidence against the model with larger AIC and BIC. Take, for instance, Tables 1 and 2 where in all cases the less favored model is the  $\Lambda$ CDM. For  $\Delta AIC$  and  $\Delta BIC$  in the range 6 – 10 one speaks of “strong evidence” against the

$\Lambda$ CDM, and hence in favor of the nonstandard models being considered. This is typically the situation for the RVM and  $Q_{dm}$  vacuum models in Table 2 and for the three  $w$ DVMs in Table 1. Neither the XCDM nor the  $Q_\Lambda$  vacuum model attain the “strong evidence” threshold in Tables 1 or 2. The XCDM parametrization, which is used as a baseline for comparison of the dynamical DE models, is nevertheless capable of detecting significant signs of dynamical DE, mainly in Table 1 (when the Riess et al. local measurement of  $H_0$  [12] – call it  $H_0^{\text{Riess}}$  – is excluded), but not so in Table 2 (where  $H_0^{\text{Riess}}$  is included). In contrast, model  $Q_\Lambda$  does not change much from Table 1 to Table 2.

In actual fact, the dynamical vacuum model  $Q_\Lambda$  tends to remain always fairly close to the  $\Lambda$ CDM. Its dynamics is weaker than that of the main DVMs (RVM and  $Q_{dm}$ ). Being  $|\nu_i| \ll 1$  for all the DVMs, the evolution of its vacuum energy density is approximately logarithmic:  $\rho_\Lambda^{\text{III}} \sim \rho_{\Lambda 0}(1 - 3\nu_\Lambda \ln a)$ , as it follows from (13) with  $\epsilon = 0$ . Thus, it is significantly milder in comparison to that of the main DVMs, for which  $\rho_\Lambda^{\text{I,II}} \sim \rho_{\Lambda 0} [1 + (\Omega_m^0/\Omega_\Lambda^0)\nu_i(a^{-3} - 1)]$ . The performance of  $Q_\Lambda$  can only be slightly better than that of  $\Lambda$ CDM, a fact that may have been unnoticed in previous studies – see [25, 35–37] and references therein.

According to the same jargon, when  $\Delta\text{AIC}$  and  $\Delta\text{BIC}$  are both above 10 one speaks of “very strong evidence” against the disfavored model ( $\Lambda$ CDM), wherefore in favor of the alternative ones. It is certainly the case of the RVM and  $Q_{dm}$  models in Table 1, which are singled out as being much better than the  $\Lambda$ CDM in their ability to describe the overall observations. From Table 1 we can see that the best-fit values of  $\nu_i$  for these models are secured at a confidence level of  $\sim 3.8\sigma$ . These two models are indeed the most conspicuous ones in our entire analysis, and remain strongly favored even if  $H_0^{\text{Riess}}$  [12] is included (cf. Table 2). In the last case, the best-fit values of  $\nu_i$  for the two models are still supported at a fairly large c.l. ( $\sim 3.2\sigma$ ), showing that the dynamical vacuum is a real option.

In Fig. 1 we confront the various models with the LSS data when the local measurement  $H_0^{\text{Riess}}$  is not included in our fit. The differences can be better appraised in the plot on the right, where we observe that the RVM and  $Q_{dm}$  curves stay significantly lower than the  $\Lambda$ CDM one (hence matching better the data than the  $\Lambda$ CDM), whereas those of XCDM and  $Q_\Lambda$  remain in between.

Concerning the  $w$ DVMs, namely the quasi-vacuum models in which an extra parameter is at play (the EoS parameter  $w$ ), we observe a significant difference as compared to the DVMs (with vacuum EoS): they *all* provide a similarly good fit quality, clearly superior to that of the  $\Lambda$ CDM (cf. Tables 1 and 2) but below that of the main DVMs (RVM and  $Q_{dm}$ ), whose performance is outstanding.

In Table 3, in an attempt to draw our fit nearer and nearer to  $H_0^{\text{Riess}}$  [12], we test the effect of ignoring the LSS structure formation data, thus granting more freedom to the fit parameter space. We perform this test using the  $\Lambda$ CDM and models ( $w$ )RVM and ( $w$ ) $Q_\Lambda$  (i.e. I and III, using vacuum and quasi-vacuum options), and we

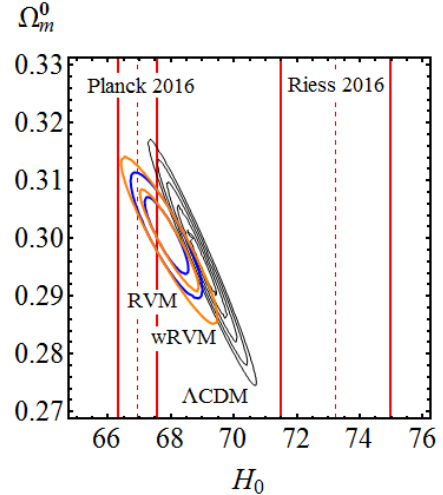


Fig. 3: Contour plots for RVM (blue) and  $w$ RVM (orange) up to  $2\sigma$ , and for the  $\Lambda$ CDM (black) up to  $5\sigma$  in the  $(H_0, \Omega_m^0)$ -plane, for the case when the local  $H_0$  value of Riess et al. [12] is included in the fit (cf. Table 2). When all data are used, any attempt at reaching the  $H_0^{\text{Riess}}$  neighborhood enforces to pick too small  $\Omega_m^0 < 0.27$  through extended contours beyond  $5\sigma$  c.l. We also observe that the two ( $w$ )RVMs are more compatible with the Planck range than the  $\Lambda$ CDM. All contours have been obtained after marginalizing over the remaining fitting parameters.

fit them to the CMB+BAO data only. We can see that the fit value for  $h = H_0/100$  increases in all starred scenarios (i.e. those involving the  $H_0^{\text{Riess}}$  data point in the fit), and specially for the cases Ia and IIIa in Table 3. Unfortunately they carry  $\nu_i < 0$  and  $w < -1$  (and hence imply phantom-like DE); and, what is worse, the agreement with the LSS data is ruined (cf. Fig. 2) since the corresponding curves are shifted too high (beyond the  $\Lambda$ CDM one). In the same figure we superimpose one more scenario, called IIIb, corresponding to a rather acute phantom behavior ( $w = -1.184 \pm 0.064$ ). The latter was recently explored in [25] so as to maximally relax the  $H_0$  tension. Unfortunately, we find that its associated LSS curve is completely strayed since it fails to minimally describe the  $f\sigma_8$  data points. Finally, in Fig. 3 we show that in the context of Table 2 (i.e. when  $H_0^{\text{Riess}}$  is included together with all the remaining data – LSS too) it becomes impossible to getting closer to that local measurement unless we go beyond the  $5\sigma$  contours and reach a too low value  $\Omega_m^0 < 0.27$ .

**Conclusions.** – We conclude that the current cosmological data disfavors the  $\Lambda = \text{const.}$  hypothesis in a very significant way. We also find that the main  $w$ DVMs used to probe the dynamical vacuum signature can cope with the Riess et al. local measurement  $H_0^{\text{Riess}}$  [12] and still provide a much better fit than the concordance model at  $\sim 3\sigma$  c.l. Such statements are firmly supported by Akaike and Bayesian criteria. However, the same criteria also tell us that the fit quality to the overall SNIa+BAO+ $H(z)$ +LSS+CMB cosmological data increases to the maximum level only when the local  $H_0^{\text{Riess}}$  measurement is not taken into account. In other words,

the CMB determination of  $H_0$  is clearly preferred. We demonstrate that not only the CMB and BAO, but also the LSS data, are essential to grant these results. If such data are not considered in the fit analysis, the models tend to accommodate the  $H_0^{\text{Riess}}$  measurement only at the expense of a phantom-like dynamical behavior of the DE, what amounts to destroy the agreement with the structure formation data. When the LSS data are restored, an excellent quality fit to the overall observations can be achieved, with no trace of phantom dynamical DE energy. In the absence of the local  $H_0^{\text{Riess}}$  measurement, the fit quality further increases in favor of the main dynamical vacuum models at  $\sim 4\sigma$  c.l. This result is bolstered by outstanding records of the information criteria (rendering  $\Delta\text{AIC} > 10$  and  $\Delta\text{BIC} > 10$ ) in favor of the main DVMs and against the concordance model. In short, we contend that significant signs of dynamical vacuum energy are encoded in the current cosmological data, which the standard  $\Lambda\text{CDM}$  model is unable to accommodate.

\*\*\*

We are partially supported by FPA2013-46570 (MICINN), Consolider CSD2007-00042, 2014-SGR-104 (Generalitat de Catalunya) and MDM-2014-0369 (ICCUB).

## REFERENCES

- [1] RIESS A. G. *et al.*, *Astron. J.*, **116** (1998) 1009.
- [2] PERLMUTTER S. *et al.*, *Astrophys. J.*, **517** (1999) 565.
- [3] WEINBERG S., *Rev. Mod. Phys.*, **61** (1989) 1.
- [4] PEEBLES P. J. E., *Principles of Physical Cosmology* (Princeton Univ. Press, Princeton) 1993.
- [5] ADE P. A. R. *et al.*, (Planck Collaboration): Planck 2015 results. XIII, *Astron. Astrophys.*, **594** (2016) A13.
- [6] PEEBLES P. J. E. and RATRA B., *Rev. Mod. Phys.*, **75** (2003) 559.
- [7] AMENDOLA L. and TSUJIKAWA S., *Dark Energy* (Cambridge Univ. Press, Cambridge) 2010 and 2015.
- [8] SANDAGE, A., *Astrophys. J.*, **133** (1961) 355.
- [9] TAMMANN G. A. and SANDAGE A., The Hubble Constant and HST. In: Macchetto F. (eds) *The Impact of HST on European Astronomy. Astrophysics and Space Science Proceedings*, (Springer, Dordrecht) (2010) 289.
- [10] TAMMANN G. A. and REINDL B., *IAU Symp.*, **289** (2013) 13; *Astron. Astrophys.*, **549** (2013) A136.
- [11] AGHANIM N. *et al.*, (Planck Collaboration): Planck 2016 intermediate results. XLVI, *Astron. Astrophys.*, **596** (2016) A107.
- [12] RIESS A. G. *et al.*, *Astrophys. J.*, **826** (2016) 56.
- [13] RIESS A. G. *et al.*, *Astrophys. J.*, **730** (2011) 119, Erratum: *Astrophys. J.*, **732** (2011) 129.
- [14] PADMANABHAN T., *Phys. Rept.*, **380** (2003) 235.
- [15] SOLÀ J., *J. Phys. Conf. Ser.*, **453** (2013) 012015.
- [16] BAADE W., *Astrophys. J.*, **100** (1944) 137.
- [17] TAMMANN G. A., *Publ. of Astron. Soc. Pacific*, **108** (1996) 1083.
- [18] CHEN G. and RATRA B., *Publ. Astron. Soc. Pac.*, **123** 1127 (2011).
- [19] BETHAPUDI S. and DESAI S., *Eur. Phys. J. Plus*, **132** (2017) 78.
- [20] BERNAL J. L., VERDE L. and RIESS A. G., *JCAP*, **1610** (2016) 019.
- [21] SHAFIELOO A. and HAZRA D. K., *JCAP*, **1704** (2017) 012.
- [22] CARDONA W., KUNZ M. and PETTORINO V., *JCAP*, **1703** (2017) 056.
- [23] NESSERIS S., PANTAZIS G. and PERIVOLAROPOULOS L., *Tension and constraints on modified gravity parametrizations of  $G_{\text{eff}}(z)$  from growth rate and Planck data*, arXiv:1703.10538.
- [24] VALENTINO E. D., MELCHIORRI A., LINDER E. V. and SILK J., *Constraining Dark Energy Dynamics in Extended Parameter Space*, arXiv:1704.00762.
- [25] VALENTINO E. D., MELCHIORRI A. and MENA, O., *Can interacting dark energy solve the  $H_0$  tension?*, arXiv:1704.08342.
- [26] SOLÀ J., GÓMEZ-VALENT A. and DE CRUZ PÉREZ J., *Astrophys. J.*, **811** (2015) L14.
- [27] SOLÀ J., GÓMEZ-VALENT A. and DE CRUZ PÉREZ J., *Astrophys. J.*, **836** (2017) 43.
- [28] SOLÀ J., GÓMEZ-VALENT A. and DE CRUZ PÉREZ J., *Mod. Phys. Lett.*, **A32** 1750054.
- [29] SOLÀ J., *Int. J. Mod. Phys. A*, **31** (2016) 1630035.
- [30] SOLÀ J., DE CRUZ PÉREZ J. and GÓMEZ-VALENT A., *Towards the firsts compelling signs of vacuum dynamics in modern cosmological observations*, arXiv:1703.08218; SOLÀ J., DE CRUZ PÉREZ J., GÓMEZ-VALENT A. and NUNES R. C., *Dynamical Vacuum against a rigid Cosmological Constant*, arXiv:1606.00450.
- [31] WANG Y. and DAI M., *Phys. Rev.*, **D94** (2016) 083521.
- [32] TURNER S. M. and WHITE M., *Phys. Rev. D*, **56** (1997) R4439.
- [33] SOLÀ J. and GÓMEZ-VALENT A., *Int. J. Mod. Phys.*, **D24** (2015) 1541003.
- [34] SOLÀ J., *J. Phys. A*, **41** (2008) 164066.
- [35] SALVATELLI V. *et al.*, *Phys. Rev. Lett.*, **113** (2014) 181301.
- [36] MURGIA. R., GARIAZZO S. and FORNENGO N., *JCAP*, **1604** (2016) 014.
- [37] LI. Y. H., ZHANG J. F. and ZHANG X. , *Phys. Rev. D*, **93** (2016) 023002.
- [38] LIMA J. A. S., BASILAKOS S. and SOLÀ J., *MNRAS*, **431** (2013) 923.
- [39] GÓMEZ-VALENT A., SOLÀ J. and BASILAKOS S., *JCAP*, **1501** (2015) 004.
- [40] GÓMEZ-VALENT A. and SOLÀ J., *MNRAS*, **448** (2015) 2810
- [41] GIL-MARÍN *et al.*, *MNRAS*, **465** (2017) 1757.
- [42] AKAIKE H., *IEEE Trans. Autom. Control*, **19** (1974) 716.
- [43] SCHWARZ G., *Annals of Statistics*, **6** (1978) 461.
- [44] KASS R. E. and RAFTERY A., *J. Amer. Statist. Assoc.*, **90** (1995) 773.
- [45] BURNHAM K. P. and ANDERSON. D. R., *Model selection and multimodel inference* (Springer, NY) 2002.